Pre-strain History Effect on Ductile Fracture

P. A. Eikrem[1,a], Z. L. Zhang[1,b], E. Østby[2,b] and B. Nyhus[2,d]

[1]Dept. of Structural Engineering, Norwegian University of Science and Technology (NTNU), 7491 Trondheim, Norway

[2]SINTEF Materials and Chemistry, N-7465 Trondheim, Norway

[a]Currently at StatoilHydro ASA, Norway, pale@StatoilHydro.com, [b]zhiliang.zhang@ntnu.no, [c]erling.ostby@sintef.no, bard.nyhus@sintef.no

Keywords: Ductile fracture, complete Gurson model, pre-strain history, strain hardening

Abstract. Fracture mechanics is mainly developed and verified for monotonic loadings. There are many scenarios where structural components are subject to a pre-strain history and it is not clear whether and how the effect of the pre-strain history can be taken into account in subsequent failure assessment. This paper focuses on the effect of plastic pre-strain history on ductile fracture resistance. Single edge notched tension (SENT) specimens are selected for the numerical study and the crack is assumed to exist before a pre-strain history was applied. The complete Gurson model has been applied to simulate the ductile fracture behavior. The results show that a plastic pre-strain history can reduce the fracture resistance *R* significantly and neither the history-independent resistance model nor material-memory resistance model existing in the literature can be used to describe the pre-strain history effect. Based on the numerical results an approximate history-dependent resistance model is proposed.

Introduction

There are many engineering scenarios where steel components are subject to a plastic pre-strain history, such as pipe reeling [1]. The pre-strain history will not only modify the yield stress and hardening, but also influence the fracture and fatigue behavior. Eikrem et al. [1] have recently found that a plastic pre-strain history can significantly increase the crack tip stress triaxiality and thus enhance the possibility for cleavage fracture. The effect of pre-strain history on the crack tip constraint decreases with the increase in external loading. The effect of pre-strain history on ductile fracture behavior has received relatively little attention in the literature and today's recommended practice ignores the pre-strain effect [2]. A numerical study is carried out in this paper to investigate the effect of a pre-strain history on ductile fracture resistance curve.

It is known that ductile crack growth in metals is a result of nucleation, growth and coalescence of micro voids. In this study, the complete Gurson model [3] has been utilized in this study. In the complete Gurson model, the critical void volume fraction is determined automatically by a plastic limit load criterion. 2D single edge notched tension (SENT) specimens are selected for this study. It has been demonstrated by Nyhus et al. [4] that the SENT specimen is a good representation of the pipe sections in terms of fracture toughness measurement. The problem considered is limited to a single pre-strain cycle, either symmetrical or non-symmetrical. Symmetrical pre-strain cycles with amplitudes up to 0.55% nominal strain have been analyzed. The non-symmetrical pre-strain cycles consist of an elongation up to 0.6% nominal strain followed by a compression down to about the initial specimen length. After the pre-strain cycle the specimen was re-loaded by tension. In the following the finite element models and the complete Gurson model will be briefly introduced, which will be followed by the main numerical results. The paper is closed with conclusions and summary.

Finite Element Model

Figure 1 shows the SENT specimen geometry and the finite element mesh used. The crack size (*a*) is 4 mm, specimen width (*w*) is 28 mm and half length (*L*) is 115 mm. Results for the cases with different *a/w* ratios can be found in [5]. A remote homogenous displacement controlled boundary condition (clamped) was applied. Because of the symmetry, half of the SENT specimen has been modeled in the finite element analyses. Four-node 2D plane strain elements were used. Close to the crack tip a region with uniform mesh size (4.8 mm ahead of the initial crack tip and 0.7 mm above the symmetrical line) is used to simulate the ductile crack growth. The element size is 0.1x0.1 mm in this local region. ABAQUS was used and nonlinear geometry effects (NLGEOM) are accounted for in the analyses. A rigid analytical plate is defined in the model to model the contact of the crack faces. Crack tip opening displacement (CTOD) has been chosen as the fracture parameter for describing the resistance behavior.

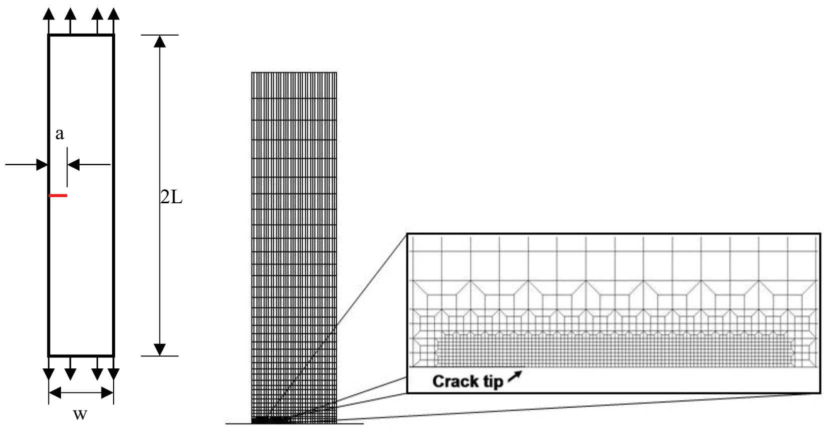

Fig. 1 Finite element model and meshes

Complete Gurson model

With the introduction of the so-called critical void volume fraction, the Gurson-Tverggard-Needleman model [7,8] can consider the effect of void coalescence. However, the model lacks a physical mechanism-based coalescence criterion. Application of the Gurson model as a predictive tool using realistic microvoid parameters demands a void coalescence criterion. Zhang and Niemi [6] have demonstrated that the plastic-limit load based coalescence model by Thomason [9] is easy to implement and very accurate compared with the finite element results. It has been shown that the Thomason plastic limit load model with certain modifications can be used to predict the coalescence of rather general cases with non-spherical voids and non-uniform void spacing [10,11].

By combing the Gurson-Tvergaard-Needleman model for void growth and Thomason's plastic limit load model for coalescence a so-called complete Gurson model has been proposed by Zhang et al. [3]. One of the important advantages of the complete Gurson model is that there is no need to select or determine the critical void volume fraction before hand. The critical void volume fraction is not a material parameter any more. It is a result of plastic deformation and is determined automatically by the plastic-limit load model.

The yield function of the Gurson-Tvergaard-Needleman model [7-8] has the following form:

$$\phi\left(q,\sigma_f,f,\sigma_m\right)=\frac{q^2}{{\sigma_f}^2}+2q_1 f\cosh\left(\frac{3q_2\sigma_m}{2\sigma_f}\right)-1-\left(q_1 f\right)^2=0 \tag{1}$$

where f is the void volume fraction, σ_m is the mean stress, q is the von Mises stress, σ_f the flow stress. q_1 and q_2 are parameters introduced by Tvergaard [7,8]. For 2D plane strain problem, Thomason's plastic limit load criterion states that coalescence occurs when the following condition is satisfied:

$$\frac{\sigma_1}{\sigma_f}=\frac{0.3}{r/(R-r)}+0.6 \tag{3}$$

In Equation (3) σ_1 is the maximum principal stress, r and R are current average void radius and intervoid distance which can be calculated from the current principle strains. Readers are referred to [3] for a full account of the complete Gurson model.

The post-coalescence deformation behavior of the Gurson model is numerically simulated by an artificial acceleration of void growth, as suggested by Tvergaard and Needleman [8]:

$$f^*=\begin{cases} f & for \quad f\le f_c \\ f_c+\dfrac{f_u^*-f_c}{f_F-f_c}\left(f-f_c\right) & for \quad f>f_c \end{cases} \tag{4}$$

where $f_u^*=1/q_1$ and f_F is the void volume fraction at the end of void coalescence, $f_F=0.15+2f_0$, where f_0 is the initial void volume fraction. When the coalescence started and $f>f_c$, f^* replaces f in Equation 1. Figure 2 shows the mean critical void volume fraction in front of the crack tip of a SENT specimen determined by the complete Gurson model. It should be noted that the critical void volume fraction determined by the complete Gurson model in the present study is around 2-3%. The critical void volume fraction can be fitted by a polynomial function of the initial void volume fraction: $f_c=-558.79f_0^2+5.7263f_0+0.0223$.

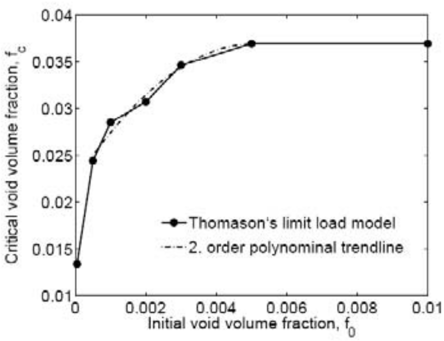

Fig. 2 Mean critical void volume fraction in front of a SENT specimen versus initial volume fraction determined by the Complete Gurson model, n=0.05.

A model material with the following power law hardening model has been used in the numerical study:

$$\sigma_f = \sigma_0 \left(1 + \frac{\varepsilon^p}{\varepsilon_0}\right)^n \tag{1}$$

where σ_f is the flow stress, σ_0 is the yield stress, ε^p is the equivalent plastic strain , ε_0 is the yield strain and n is the hardening exponent. In all the analyses σ_0 =400MPa and the elastic properties Young's modulus E = 200GPa and Poisson ratio ν = 0.3 are fixed.

Pre-strain Effect on Resistance Curves

Fracture mechanics is mainly developed and verified for monotonic loading. It is not clear how the fracture mechanics can be extended for cyclic loading. Ernst et al. [12] recently proposed two models, a history-independent *R* curve and a material-memory *R* curve, to describe the resistance behaviour after a pre-strain history, Figure 3. Today's recommended practice [2] does not consider the effect of pre-strain history and the history-independent resistance model is used. In the history-independent resistance model the shape of the resistance curve is the same for all loading cycles, irrespective of the pre-strain history. If crack extension takes place in the current cycle the resistance curve is shifted towards the current crack length before the next cycle starts. In the material-memory resistance model the resistance curve does not shift to a new origin from one cycle to another one. The crack driving force achieved in the previous cycle needs to be reached in the next cycle in order for further crack extension to take place. Although it was concluded that material-memory *R* curve seems to better fit their experimental results, the effect of pre-strain history on the ductile fracture resistance is not well understood.

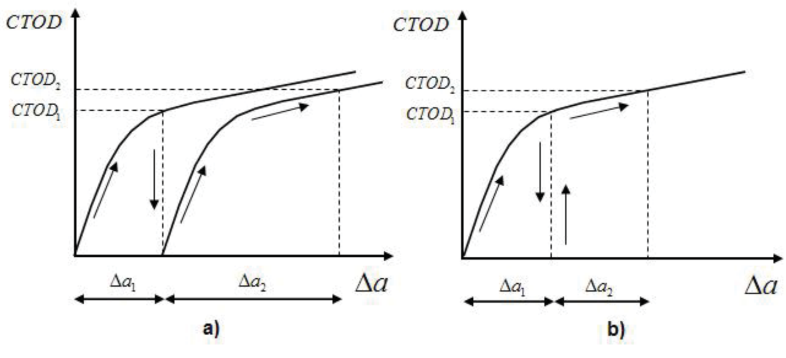

Figure 3 a) History-independent *R* curve and b) material-memory *R* curve [12].

SENT specimens with both a symmetric and non-symmetric pre-strain cycle have been analyzed with the complete Gurson model. For each SENT specimen three pre-strain cycles have been analyzed in addition to the case with monotonic tension. In all the cases with a pre-strain history the specimens were loaded by tension first. Reverse loading started at different nominal strain levels. The fracture resistance curves for the four cases with symmetrical pre-strains are shown in Figure 4a for n=0.05. Figure 4a shows when the pre-strain is 0.2% there is already about 40% reduction in the initiation toughness in the re-tension loading. It is interesting to note that the resistance curve in the re-tension looks rather similar to the resistance of the material with monotonic loading. For the case with pre-strain 0.3% there is no crack growth at the end of the pre-tension. However, crack growth starts at approximately zero CTOD in the re-tension. There is about 0.2 mm crack growth in the pre-tension loading for the case with 0.4% pre-strain. The initiation CTOD for the case with 0.4% pre-strain is the same as the case with 0.3% pre-strain and close to zero.

Similar analysis has been carried out for the same SENT specimen with a high hardening material n=0.1. The general trend is the same. Increasing the pre-strain level will reduce both the initiation as well as the fracture resistance. For the high strain hardening material (n=0.1) a larger pre-strain level is needed to induce the crack growth in the pre-strain cycle. The effect of plastic strain hardening on the fracture resistance can not be easily verified by experiments and contradictory results have been reported in the literature. A systematic study on this topic will be reported elsewhere.

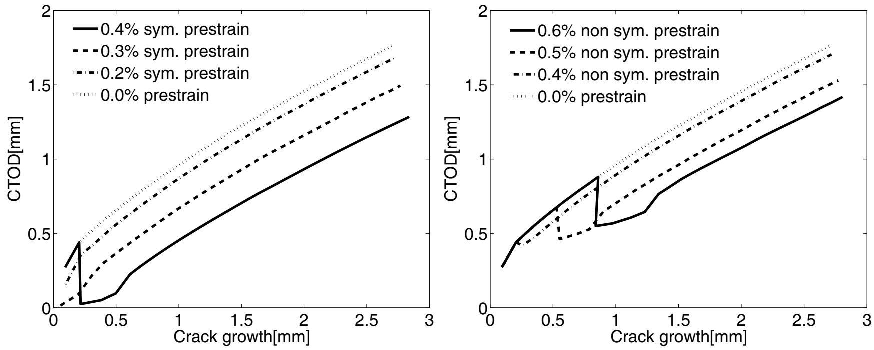

Figure 4 Effect of pre-strain history on the ductile resistance curve for the case with n=0.05 and f_0=0.005. a) Symmetrical pre-strain history and b) non-symmetrical pre-strain history.

The effect of a non-symmetrical per-strain history on the ductile fracture resistance is shown in Figure 4b. The specimen is loaded in tension to a specified pre-strain level and then unloaded to about the initial specimen length without further compression. Three pre-strain levels are analyzed. During the re-tension, crack growth starts at a lower CTOD than the CTOD at the end of the pre-strain cycle, but greater than the initiation CTOD in the monotonic loading.

Both the 0.4% symmetrical pre-strain and 0.4% non-symmetric pre-strain cases have the same amount of crack growth but different degree of compression in the pre-strain cycle. It can be observed from Fig. 4 that the fracture resistance curves for the two cases are significantly different. The fracture resistance curve in the re-tension loading for the 0.4% symmetrical pre-strain case starts at almost zero CTOD while there is only a slight down shift from the monotonic resistance curve for the non-symmetrical case. The results indicate that the compression in the pre-strain history plays a detrimental role in the fracture resistance.

The effects of pre-strain on the fracture resistance for the symmetrical cases with n=0.05 and 0.1 and also the non-symmetrical case with n=0.05 are re-plotted in Fig. 5. The CTOD at 1 mm crack growth for the three cases are plotted against the pre-strain levels. It can be clearly seen that the reduction of fracture toughness is more significant for the low hardening material (n=0.05) than the strong hardening material (n=0.1). For the same material the effect of a non-symmetric pre-strain cycle is generally much smaller than the symmetrical pre-strain cycle.

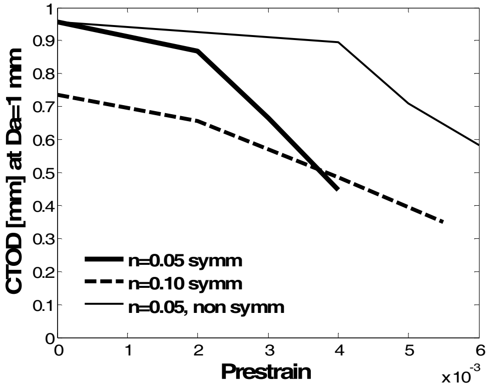

Fig. 5 Effect of pre-strain on the reduction of CTOD at 1 mm crack growth.

The results shown in Fig. 4-5 indicate that the resistance curves depend on the pre-strain history. The existing models proposed by Ernst can not be used to describe the present results. It can be observed from Fig. 4-5 that the pre-strain cycle influences the initiation toughness in the re-tension loading. However, after a small amount of crack growth the resistance curve with a pre-strain history clearly resembles the resistance of the one with monotonic loading. Based on this observation, a new resistance curve model to take the pre-strain history into consideration is proposed. The new model is called history dependent resistance model and is schematically shown in Fig. 6.

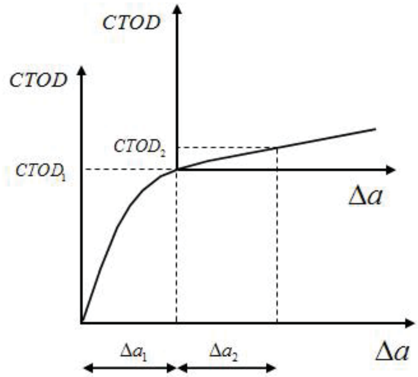

Figure 6 Proposed history-dependent R curve.

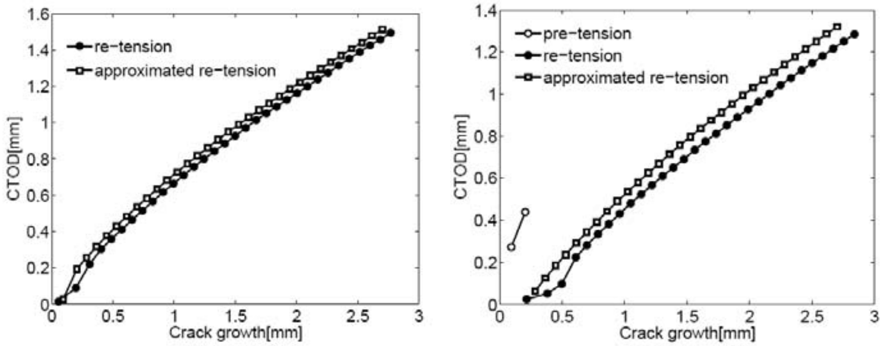

Fg. 7 Comparison of the approximated and numerical resistance curves after a symmetrical pre-strain cycle a) 0.3% and b) 0.4%. n=0.05 and a/w=0.14.

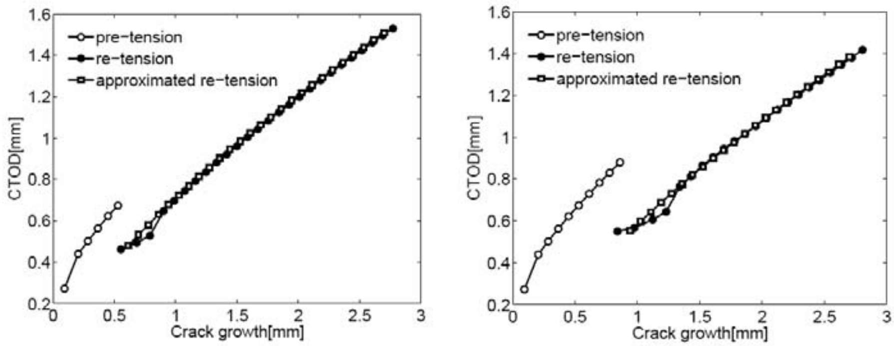

Fg. 8 Comparison of the approximated and numerical resistance curves after a non-symmetrical pre-strain cycle a) 0.5% and b) 0.6%. n=0.05 and a/w=0.14.

In the new resistance model, the point on the reference curve where the first pre-tension cycle ended becomes the new origin of the resistance curve in the re-tension loading. The resistance curves constructed according to the new history-dependent R curve model are compared with the resistance curves directly from the finite element analyses in Fig. 7 and 8 for the symmetrical and non-symmetrical pre-strain cases, respectively. It can be seen that there is a reasonable agreement between the approximated resistance curves for both the symmetrical and non-symmetrical curves.

Summary

Fracture mechanics is mainly developed and verified for monotonic loading. The present results show that a plastic pre-strain history can significantly reduce the subsequent fracture resistance. The subsequent fracture resistance curve depends on the nature and level of pre-strains and strain hardening of the material. Neither the history-independent nor the material memory resistance curve models can be used to describe the present results. The reduction of fracture resistance in the re-tension loading is controlled by the degree of compression experienced in the pre-strain cycle. When the compression is severe enough the crack initiation CTOD in the re-tension loading will be close to zero. Apart from a small range close to the initiation in the re-tension the fracture resistance curvature and shape are similar to the resistance curve in the monotonic loading. A new history-dependent resistance model is proposed to predict the fracture resistance curve including the effect of pre-strain. Experimental validation of the model is planned in the near future.

References

[1] P. A. Eikrem, Z. L. Zhang and B. Nyhus, Effect of plastic prestrain on the crack tip constraint of pipeline steels, Int. J of Pressure Vessels and Pipings V84 (2007) p.708.

[2] S. Wastberg, , H. Pisarki, and B Nyhus,. Guidelines for engineering critical assessments for pipelines installation methods introducing cyclic plastic strain. *In International Conference on Offshore Mechanics and Arctic Engineering* (OMAE 2004), 2004, Vancouver, Canada.

[3] Z. L. Zhang, C. Thaulow and J. Ødegård, A complete Gurson model approach for ductile fracture, *Engineering Fracture Mechanics*, **67** (2000) p.155.

[4] B. Nyhus, M. L. Polanco, and O. Ørjasæther, SENT specimens an alternative to SENB specimens for fracture mechanics testing of pipelines, *Proceedings of the 22nd International Conference on Offshore Mechanics and Arctic Engineering(OMAE 2002), Jun 8-13 2001*, Cancun, Mexico 2003, pp. 259-266.

[5] P. A. Eikrem, Z. L. Zhang E. Østby, and B. Nyhus, Numerical study on the effect of pre-strain history on ductile fracture resistance by using the complete Gurson model, to appear at Engineering Fracture Mechanics.

[6] Z. L. Zhang and E. Niemi, A new failurecriterion for the Gurson-Tvergard dilatational constitutive model, *Int. J. Fracture,* V70 (1995) p.321.

[7] V. Tvergaard, On localization in ductile materials containing spherical voids, *Int. J. Fracture*, **18** (1982) p.237.

[8] V. Tvergaard and A. Needleman, Analysis of the cup-cone fracture in a round tensile bar, *Acta Metall*, **32** (1984) 157.

[9] P. F. Thomason, Ductile fracture of metals, Oxford, Pergamon Press, 1990

[10] A. A. Benzerga, Micromechanics of coalescence in ductile fracture, *J. Mech. Phys. Solids*, V50 (2002) p.1331.

[11] T. Pardoen and W. Hutchinson, An extended model of void growth and coalescence, *J. Mech. Phys. Solids*, V48 (2000) p.2467.

[12] H. Ernst, R. E. Bravo, F. Daguerre and A. Izquierdo, Strain history effects on fracture mechanics parameters - application to reeling, *Proceedings of the 24th International Conference on Offshore Mechanics and Arctic Engineering* (OMAE 2005), June 12-17, 2005, Halkidiki, Greece.